



Isolation and Characterisation of Akuammine from the Seed of *Parinari curatellifolia* and its Molecular Dynamics in Angiotensin -1- Converting Enzyme Inhibition

Olamide O. Crown^a, Samson O. Famuyiwa^{b*}, Olanrewaju S. Olayeriju^c, Mary T. Olaleye^d, Victor I. Ogungbe^a Derek T. Ndinteh^e.

^aDepartment of Chemistry, College of Sciences, University of Alabama, Huntsville Alabama, 35899, USA.

^bDepartment of Chemistry, Faculty of Science, Obafemi Awolowo University, Nigeria.

^cDepartment of Biochemistry, Olusegun Agagu University of Science and Technology, Okitipupa, Ondo state, Nigeria.

^dDepartment of Biochemistry, Phytomedicine, Toxicology and Pharmacology Unit, School of Sciences, Federal University of Technology, Akure, Nigeria.

^eDepartment of Chemical Sciences, Faculty of Sciences, University of Johannesburg, Doornfontein campus, South Africa.

ARTICLE INFO

Article history:

Received 16 March 2024

Revised 10 May 2024

Accepted 17 May 2024

Published online 01 June 2024

Copyright: © 2024 Crown *et al.* This is an open-access article distributed under the terms of the [Creative Commons Attribution License](https://creativecommons.org/licenses/by/4.0/), which permits unrestricted use, distribution, and reproduction in any medium, provided the original author and source are credited.

ABSTRACT

Over the years, isolated compounds from medicinal plants have been lead candidates in drug discovery and they are useful therapeutic aid to patients. This work isolated a compound from the seed of *Parinari curatellifolia* and investigated its inhibitory potential and mechanism on angiotensin-1-converting enzyme (ACE1). The methanolic extract of the seed was subjected to chromatographic techniques and yielded a white, crystalline solid. Structural elucidation of the compound was carried out using NMR and MS spectroscopic techniques. The use of N-(3-[2-furyl-acryloyl]-Phe-Gly-Gly) (FAPGG) as an enzyme substrate and the Michealis-Menten method in this study showed how sensitive and fast ACE1 could be inhibited. Inhibition mechanism was explored using the Lineweaver-Burk model, and IC₅₀ was determined using Cheng-Prusoff empirical analysis. Molecular interaction with ACE1 was investigated computationally. NMR and MS spectroscopy showed the compound to be Akuammine, with 26 protons, 22 carbons, 2 nitrogen, and 4 oxygen atoms and chlorinated molecular ion peak at m/z 417.1593. Akuammine exhibited an IC₅₀ of 8.5 μM and displayed mixed type inhibition. Molecular dynamics simulations indicated strong interaction at the allosteric site of ACE1, primarily through hydrophobic interactions. Akuammine demonstrated an ability as a template for antihypertensive agent. This ability may contribute to the ethno botanical uses of *Parinari curatellifolia* seed.

Keywords: Akuammine, Angiotensin converting enzyme, Antihypertension, *Parinari curatellifolia*

Introduction

Hypertension remains a significant global health concern, posing challenges to effective management despite various treatment options. The recent surge in its incidence in Africa, attributed to factors such as stress and lifestyle changes, underscores the urgency to explore novel therapeutic avenues.¹ The regulation of blood pressure homeostasis involves complex cellular and humoral mechanisms, often compromised by stressors like oxidative stress and disease complications, leading to elevated blood pressure levels.² Among the key regulators of peripheral vascular resistance, angiotensin II stands out as a potent vasoconstrictor, primarily activated by angiotensin I converting enzyme (ACE1).^{3,4,5} The inhibition of ACE has emerged as an effective strategy in hypertension management, with synthetic ACE inhibitors widely prescribed despite associated adverse effects.^{6,7,8} In recent years, there has been growing interest in harnessing the therapeutic potential of natural plants for hypertension management, given their diverse bioactive compounds.

*Corresponding author. E mail: sofamuyiwa@oauife.edu.ng
Tel: 08166020238

Citation: Crown OO, Famuyiwa SO, Olayeriju OS, Olaleye MT, Ogungbe VI, Ndinteh DT. Isolation and Characterisation of Akuammine from the Seed of *Parinari curatellifolia* and its Molecular Dynamics in Angiotensin -1- Converting Enzyme Inhibition. Trop J Nat Prod Res. 2024; 8(5): 7309-7314. <https://doi.org/10.26538/tjnpr/v8i5.37>

Official Journal of Natural Product Research Group, Faculty of Pharmacy, University of Benin, Benin City, Nigeria

Notably, alkaloids, nitrogen-containing compounds abundant in the plant kingdom, have demonstrated cardioprotective properties, albeit limited investigations on ACE1 inhibition.⁹ *Parinari curatellifolia*, an indigenous African medicinal plant, boasts a rich ethnopharmacological history, with documented uses spanning wound infections, cancer, and notably, hypertension. While previous studies have highlighted the pharmacological properties of *P. curatellifolia* extracts, including ACE inhibition, the active principle responsible for these effects remains elusive.^{10,11}

Our previous research reported the cardioprotective (Crown *et al.*, 2010) antihypertensive potential¹⁰ and ACE inhibition of *P. curatellifolia* extracts,¹¹ yet the identification of the active compound(s) driving these effects remained unexplored. In this study, we aim to isolate and characterize Akuammine, a prominent alkaloid from the seeds of *P. curatellifolia*, and investigate its potential as an ACE1 inhibitor. Through molecular dynamics simulations, we seek to elucidate the mechanistic basis of Akuammine-mediated ACE1 inhibition, shedding light on its therapeutic relevance in hypertension management. This research endeavor represents a novel approach to addressing health disparities associated with hypertension, leveraging the natural bioactive compounds present in indigenous medicinal plants like *P. curatellifolia*.

Material and Methods

General

NMR spectra were measured on Bruker ARX 500 NMR spectrometer using CDCl₃ as solvent and internal standard. The mass spectra were determined on a Bruker Compact Q-TOF high resolution Compact mass spectrophotometer. For TLC, pre-coated silica gel 60F₂₅₄ plates were

used and silica gel (70-230 mesh). Compound was detected under ultra-violet (UV) lamp (254) and further visualized by spraying with vanillin-sulphuric acid solution. Angiotensin-1 converting enzyme (ACE1) and N-(3-[2-furyl] acryloyl)-Phe-Gly-Gly (FAPGG) were purchased from Sigma-Aldrich, MO, USA. Bradford Reagent and BSA were obtained from Bio-Rad Laboratories, Hercules, CA, USA.

Plant material and extraction

The seeds of *Parinari curatellifolia* (PC) were purchased at the Oba's market in Akure, Nigeria, in the month of June, 2018. Botanical identification and authentication were carried out and the voucher specimen (PC005) was deposited at the Department of Biochemistry, Federal University of Technology Akure, Nigeria.

The seeds of PC were air-dried, pulverized and extracted with 80% methanol as described by Crown *et al.*, (2017). The filtrate was dried to obtain crude extract. Furthermore, the crude extract was dissolved in methanol and the solution was filtered. The methanolic solution was concentrated *in-vacuo* to obtain the methanolic extract (135 g).

Isolation of the compound and its spectroscopic data

The extract was subjected to column chromatography. The column was subjected to isocratic elution with chloroform/methanol (12:1). Fifty-two fractions of 250 ml each was collected and concentrated to dryness. The fractions were spotted on TLC and fractions of similar RF were pooled together to obtain seven fractions. Akuammine precipitated out from fractions 6 and 7 when methanol was added. It was filtered through glass wool. It was further purified by washing the precipitate with methanol.

Akuammine

White amorphous solid; melting point (258 – 260° C), IR (KBr): ν_{\max} (cm⁻¹) 3408 (OH), 1735 (C=O) and 1599 (C=C of the benzene ring), 1464, 1276, 1257 (C-O-C of ester). ¹H and ¹³C NMR, Table 1.

Determination of ACE1 Inhibitory Activity

ACE1 catalyses the hydrolysis of N-(3-[2-furyl]acryloyl)-Phe-Gly-Gly (FAPGG) to furyl-acryloyl-phenyl-alanine (FAP) and glycyl-glycine. Hydrolysis of FAPGG resulting in a decrease in absorbance was monitored at 345 nm at 25°C using Shimadzu 1800 Double beam UV-Visible Spectrophotometer. The molar extinction coefficient difference between substrate and product of 517 cm⁻¹ M⁻¹ was used to calculate activity. The ACE1 inhibitory activity was measured according to the method of Homoliquist *et al.*, (1979)¹² with modifications reported by Crown *et al.*, (2017). The ACE1 activity was expressed as ΔA 345 nm and the ACE1 inhibition (%) was calculated using the equation (1):

$$\left[1 - \frac{\Delta A_{\text{inhibitor}}}{\Delta A_{\text{control}}}\right] \times 100 \quad (1)$$

IC₅₀ was defined as the concentration of sample required to inhibit 50% of ACE1 activity under these conditions. The molar extinction

coefficient between substrate and product was assumed to be 517 cm⁻¹ M⁻¹ at 345 nm.¹³ Protein content was determined using Bradford method.¹⁴

Determination of the Kinetic Properties of ACE1 Inhibition by extracts

The kinetic properties of ACE1 (20 mU) without or with Akuammine (15, 20 and 30 µg/ml) in total volume of 1.22 mL were determined using different concentrations of FAPGG as substrates (0.1 - 0.5 mM). The K_M and K_M' were calculated from linearization of Michaelis-Menten's equation (2);

$$\frac{1}{v_o} = \left(\frac{\alpha K_M}{v_{\max}}\right) \left[\frac{1}{S}\right] + \alpha' / v_{\max} \quad (2)$$

Where V is the volumetric reaction rate, S is the substrate concentration, K_M is the constant of Michaelis-Menten, V_{max} is the maximum reaction rate at infinite reactant concentration.

The determination of inhibition constant (K_i) was performed using equations (3) and (4);

$$\alpha = 1 + [I]/K_i \quad (3)$$

$$\alpha' = 1 + [I]/K_i' \quad (4)$$

I is the inhibitor concentration, K_i is the inhibition constant, α is the factor by which K_M changes when I occupies the enzyme, α' is the factor by which apparent K_M changes when I occupies the enzyme. The determination of dissociation constant (K_d) was performed using the Cheng- Prusoff's equation (5):

$$K_i = \frac{IC_{50}}{1 + (L/K_d)} \quad (5)$$

Where: K_i is the inhibition constant, IC₅₀ is the concentration that inhibits 50% of the enzyme, L is the free Inhibitor, K_d is the dissociation constant.

Computational methods

Protein-ligand docking studies were carried out based on the crystal structures of angiotensin 1 converting enzyme (PDB:1O86). Prior to docking, all solvent molecules and the co-crystallized ligands were removed from the structures. Molecular docking calculations for all compounds with each of the proteins were undertaken using Molegro Virtual Docker (version 6.0, Molegro ApS, Aarhus, Denmark),¹⁵ with a sphere (10 Å radius) large enough to accommodate the cavity centred on the binding sites of each protein structure in order to allow each ligand to search. The compound was allowed to bind randomly to the protein. Standard protonation states of the proteins based on neutral pH were used in the docking studies. Each protein was used as a rigid model structure; no relaxation of the protein was performed. Assignments of charges on each protein were based on standard templates as part of the Molegro Virtual Docker program; no other charges were necessary to be set. Akuammine was docked. Each ligand structure was built using Spartan '14 for Windows (version 1.1.8, Wavefunction Inc., Irvine, California).

Table 1: Proton, carbon-13 and HMBC NMR data in CDCl₃ (multiplicities in parenthesis)

Position	Proton (multiplicity)	¹³ Carbon	HMBC (¹ H to ¹³ C)	Position	Proton (multiplicity)	¹³ Carbon	HMBC (¹ H to ¹³ C)
1	-	-	-	13	-	144.9	-
2	-	103.5	-	14	2.00 (dd) 2.32 (dd)	27.4	58.0, 103.5 138.3
3	4.27 (s)	52.6	40.4	15	3.45 (s)	40.4	52.6, 73.9
4	-	-	-	16	-	58.0	-
5	2.69 (dd) 3.78 (ddd)	50.0	53.4, 54.1 53.4, 54.1	17	3.57 (d) 3.89 (d)	73.9	53.4 103.5
6	1.51 (dd) 3.36 (ddd)	29.8	53.4 50.0, 53.4, 58.0	18	1.48 (d)	13.0	120.8, 138.3
7	-	53.4	-	19	5.44 (q)	120.8	40.4, 54.1
8	-	139.7	-	20	-	138.3	-
9	6.60 (d)	111.2	144.9	21	2.91 (d) 3.96 (d)	54.1	40.4, 50.5, 52.6, 120.8 -
10	-	150.2	-	22	-	171.6	-
11	6.55 (dd)	113.7	144.9	OCH ₃	3.74 (s)	52.1	171.6
12	6.43 (dd)	110.6	139.7, 150.2	24	2.69 (s)	29.6	103.5, 144.9

For each ligand, a conformational search and geometry optimization was carried out using the MMFF force field.¹⁶ Flexible ligand models were used in the docking and subsequent optimization scheme. Variable orientations of each of the ligands were searched and ranked based on their re-rank score. For each docking simulation the maximum number of iterations for the docking algorithm was set to 1500, with a maximum population size of 30 runs per ligand. The RMSD threshold for multiple poses was set to 1.00 Å. The generated poses from each ligand were sorted by the calculated re-rank score. The homology modelling interface generates a set of putative protein structures by aligning atomic coordinates of the amino acid sequence to those of the template sequence backbone and minimising permutations of side chain orientations using the AMBER10:EHT force field with reaction field solvation.^{17,18,19} The candidate structure with the lowest RMSD deviation from the template backbone is selected and optimized using a constrained minimization. Each of the sequences was aligned to its respective template and a protein backbone constructed and superposed to the reference structures using the protein alignment tool in MOE 2014.0901.

Statistical Analysis

The data were expressed as the Mean of the triplicate determinations and the Standard Deviation (SD) or Standard error of measurements (SEM). Statistical significance was evaluated using ANOVA followed by Tukey's test for multiple comparisons. The data were also analyzed using GraphPad Prism 5 (GraphPad software, Inc., La Jolla, CA, USA). Data were fitted to either the Eq. 1-3 or the Michaelis-Menten equation using KaleidaGraph 4.5 (Synergy Software, MA, USA).

Results and Discussion

Structural elucidation of the isolated compound

The HRESIMS of the compound, Figure 1, showed a chlorinated molecular ion peak at m/z 417.1593 [M + Cl] consistent with a molecular formula $C_{22}H_{26}N_2O_4Cl$. The 1H NMR (500 MHz, $CDCl_3$) of the compound showed resonances at δ 3.74 (s), δ 2.69 (s) and δ 1.48 (d), each integrated to be three protons indicating three methyl groups with a signal at δ 3.74 to be a methoxy. A signal at δ 5.44 (q) indicated an olefinic proton. The signals in the aromatic region at δ 6.43 d ($J = 8.3$), 6.55 dd ($J = 2.4, 8.3$) and δ 6.60 d ($J = 2.4$) each integrated to be one proton suggested 1, 2 and 4 tri-substitution on benzene ring. The analyses of ^{13}C and HSQC data showed signals for twenty two carbon atoms and their respective correlations with protons (protons in parentheses) at δ 171.6, 150.2, 144.9, 139.7, 138.3, 120.8 (H (5.44 q)), 113.7 (H (6.55 dd)), 111.2 (H (6.60 d)), 110.6 (H (6.43 dd)), 103.3, 73.9

(2H (3.57 d), (3.89 d)), 58.0, 54.1 (2H (2.91 d), (3.96 d)), 53.4, 52.6 (H (4.27 s)), 52.1 (3H (3.74 s)), 50.0 (2H (2.69 dd), (3.78 ddd)), 40.4 (H (3.45 s)), 29.8 (2H (1.51 dd), (3.36 ddd)), 29.7 (3H (2.69 s)), 27.4 (2H (2.00 dd), (2.32 dd)) and 13.0 (3H (1.48 s)). The HMBC correlations were shown in Table 1. The NMR data of the isolated compound compared well with the published data by Lewin and Ménez, 1992,²⁰ thus the compound was identified as akuammine, Figure 2.

Inhibitory effect of akuammine on ACE1

The inhibitory plot of akuammine shown in Figure 3 is a sigmoidal plot. The result revealed that the ACE1 inhibition was concentration dependent. The concentration that inhibits 50% of the ACE1 was 20 $\mu g/ml$.

Kinetics of ACE1 inhibition

In the absence and presence of akuammine, the Lineweaver-Burk plot that the type of inhibition exhibited is a mixed type of inhibition as shown in the Figure 4. The kinetic parameters as shown in Table 2 showed that the K_m decreased with the values 0.716, 0.656, 0.648 $\mu g/ml$ and the V_{max} increased with the values 0.34, 0.24, 17.56 $ng/ml/min$ as the concentrations of akuammine used as inhibitors was increased from 15 to 30 $\mu g/ml$. The K_m' values of all the concentrations of akuammine were 2588.34, 2371.44, 2342.52 respectively and V_{max}' values of all the concentration were 1.518, 1.229, 63.479 $\mu g/ml/min$ respectively. The inhibition constant (K_i) and the K_i' for all concentrations of akuammine (15 to 30 $\mu g/ml$) were the same with the value of 15.03 $\mu g/ml$ and 15 $\mu g/ml$ respectively. The dissociation constant i.e., the K_d values and K_d' of all the concentration of akuammine were 0.3, 0.86, 1.44 $\mu g/ml$ and 0.3, 0.64, 0.23 respectively.

Molecular Docking Study

Figure 5 showed the binding of pose of Angiotensin-I-Converting Enzyme {ACE1 (PDB: 1O86)} with Akuammine. It showed that the binding of Akuammine to ACE1 (1O86) was on the allosteric site. The result from Table 2 revealed that binding of Akuammine to the allosteric site was more favourable because of its low binding energy obtained while binding to the active site was not favourable.

Angiotensin-I-converting enzyme (ACE) is one of the drug targets for the management of hypertension. Despite several contraindications and multiple side effects of the ACE inhibitors, drug has remained the most used in the management of high blood pressure, and physicians are left with the management of the various side effect which also is a major challenge to the health of the patient.

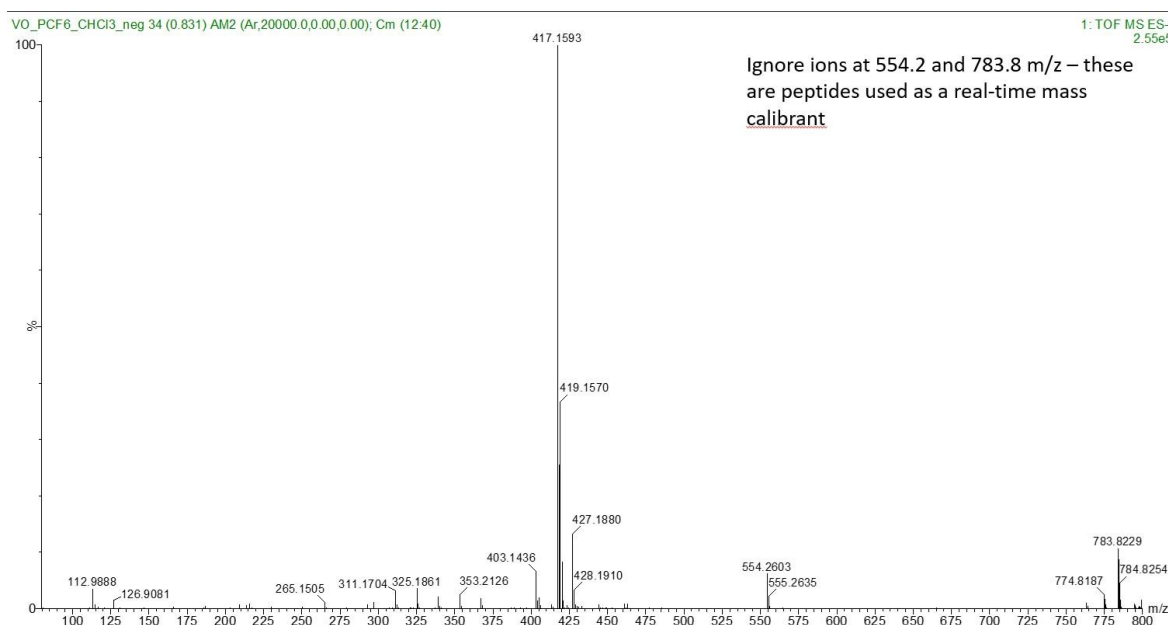


Figure 1: High resolution electron spray ionization mass spectrum of Akuammine

In this study, the concentration dependent inhibition (Figure 2) exhibited by Akuammine and IC₅₀ of 3.23 µg/ml (8.5 µM) final concentration suggested that it will be a good antihypertensive drug. Comparing with other ACE1 inhibitors, Akuammine exhibited a lower inhibition than some of the known and established antihypertensive natural products.^{11,21,22} The inhibitory plot of Akuammine was sigmoidal and was fitted to a Hill's plot rather than Michaelis-Menten plot (Figure 2). Enzyme inhibition with sigmoidal plot is a clear indication that the enzyme is allosteric in nature therefore an allosteric enzyme model was used for its interpretation. This was analysed by Hill's equation (6):

$$V_o = V_{max}[S]^{nH} / K_M^{nH} + [S]^{nH} \quad (6)$$

nH is a qualitative indication of the level of cooperativity. The Hill's plot for ACE binding to Akuammine gave a Hill coefficient (nH) greater than 1. This indicates positive cooperativity of the inhibition at site outside the active site of ACE.

The inhibition behaviour of Akuammine on ACE1 (Figure 3) gave increasing slopes and growing Y-axis intercepts with higher inhibitor concentration indicating that Akuammine is a mixed type inhibitor. The double reciprocal plot yielded a family of lines with different slopes and intercepts, and they intersect at the 2nd quadrant. The inhibitory behaviour, from the double reciprocal plot, the decrease Km and increase Vmax denoted mixed type of inhibition, this implies that the inhibitor binds to the enzyme or enzyme-substrate complex i.e., the binding of the inhibitor did not affect the binding of the substrate, but prevented product formation. This type of inhibition is unaffected by the amount of substrate unlike competitive inhibitor where increase in concentration of the substrate prevents the binding of inhibitor. Most medicinal plants exhibited this type of inhibition. Earlier study by Crown *et al.*, (2017),¹¹ reported crude extract of *P. curatellifolia* also exhibited mixed type of inhibition of ACE1. The factor α or α' describes the effect of the inhibitor on the affinity of the substrate towards the enzyme and the effect of substrate on the inhibitor affinity for the enzyme. The α and α' (Table 2) for Akuammine was not different from control which was a clear indication that the inhibitor has no effect on the affinity of substrate on inhibitor or vice-versa. In general, there is partially mixed inhibition when $\alpha < 1$, complete uncompetitive inhibition is characterized by $\alpha \ll 1$ while $\alpha > 1$ depict the enzyme binds favourably to enzyme substrate complex.

The inhibitor binding constants for enzyme (K_i) and enzyme substrate complex (K_{is}) were obtained from secondary plots; Figure 3b and c respectively. The K_{is} (21.2 µg/ml) was larger than K_i (14.3 µg/ml) indicating that the affinity for enzymes is stronger than the enzyme-substrate complex.

The Km, KI, and with enzyme-substrate complex, KIS, were obtained from the inhibition constant (K_i) was an index that defines inhibitor binding (affinity) capacity to the enzyme in order to form the enzyme-inhibitor complex and a lower value implies a higher affinity.²³ The result showed the K_i obtained was the same for the concentration of Akuammine. This suggested that the different concentrations of Akuammine had the same binding capacity to the enzyme.

The observed dissociation constant (K_d) was determined from Cheng-Prusoff's equation. K_d measured the ability of the inhibitor to dissociate from either enzyme-inhibitor or enzyme-substrate-inhibitor complex. The higher the K_d the faster the dissociation.¹¹ From the results, it was discovered that as the concentration increases, the dissociation constant also increases.

Molecular docking was carried out to further confirm the interaction between the Akuammine and the ACE1 and it revealed that the Akuammine bound on a separate site aside the active site, which clearly support the earlier claim in this study that the enzyme is an allosteric enzyme and that Akuammine bound to the allosteric site which favoured mixed type inhibition. The binding to the allosteric site was more favourable (Table 3) because it has very low re-rank, molecular docking score, but when Akuammine was forced to bind at the active site, it interacted with more amino acids than lisinopril but the docking/re-rank scored were very high (Table 3). This suggested that Akuammine favourably binds to the allosteric site. The hydrogen bond of Akuammine was mostly with water and at most with 2 amino acids whereas the hydrophobic bonding was with 4-8 amino acids. There was no electrostatic bonding interaction, all these depicts that the compound was highly hydrophobic. The physicochemical properties of the compound revealed that total polar surface area was 93. The total surface area measures the membrane permeability of compound.

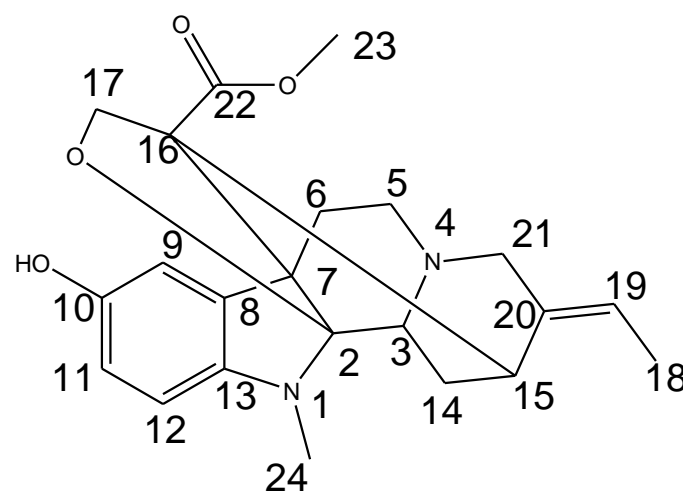


Figure 2: Structure of akuammine

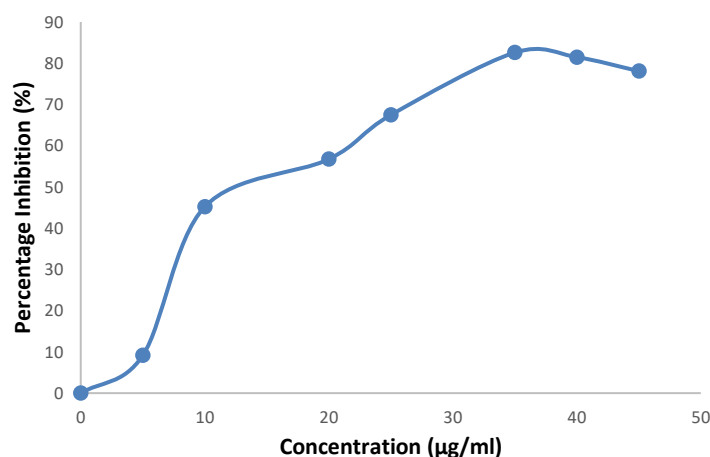


Figure 3: Inhibitory plot Akuammine on ACE1 activity

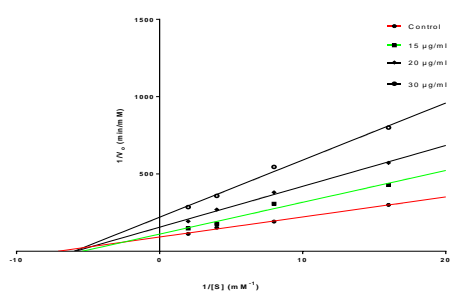
Table 2: Kinetic Parameters obtained from Lineweaver-Burk Adjustment for ACE1 Inhibition by Crude and Flavonoid-Rich Extracts

	V _{max} (µM/min)	K _m (µM)	α	α'
No extract	0.21 ± 0.00 ^a	272 ± 0.02 ^a	0.002 ± 0.01 ^a	7.23 ± 0.01 ^a
Ak (15 µg/ml)	0.17 ± 0.08 ^a	358 ± 0.04 ^b	0.002 ± 2.54 ^b	7.23 ± 3.54 ^b
AK (20 µg/ml)	0.12 ± 0.06 ^a	328 ± 0.01 ^b	0.0028 ± 1.82 ^c	7.23 ± 3.73 ^c
AK 30 µg/ml	8.78 ± 0.92 ^b	324 ± 0.00 ^b	0.002 ± 0.38 ^b	7.23 ± 5.63 ^d

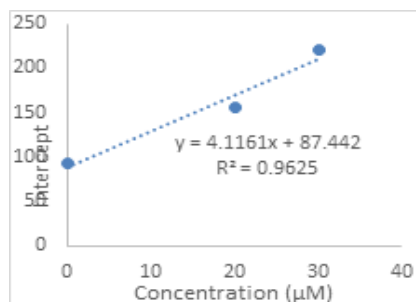
Values are expressed as mean ± SD. Values with different superscripts are significantly (P<0.05) different from each other down the column.

Table 3: The molecular interaction and Rerank score of Akuammine at the active and the allosteric site of ACE1

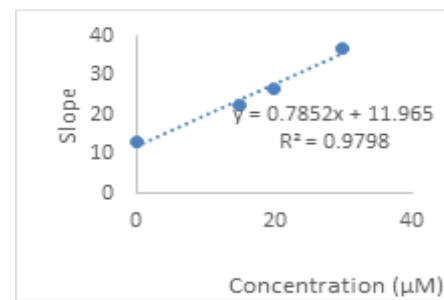
Ligand	Substrate site			Electrostatic bond	Allosteric site		
	RMS	Hydrogen bond	Hydrophobic bond		RMS	Hydrogen bond	Hydrophobic bond
Akuammine pose 1	189.7	Lys 511, Tyr 520, Gly_2000, Solvent (2473, 2569,2567,2568)	Lys 511, Tyr 520, Phe 457, Tyr 523, His 383, Ala 354, Glu 384, His 353		-67.6	Arg 124, Glu 123, Thr 92, Ile 88, Asn 85	Arg 124, Solvent (2479, 2127, 2230, 2110, 2111A, 2370, 2152)
Akuammine pose 2	152.4	Tyr 520, Asp 415, Gln 281, Solvent (2452, 2568,2569)	His 383, Tyr 520, Phe 457, Asn 415, His 513, Tyr 523, Phe 527, Glu 384, Gln 281, Ala 354, His 363		-65.3	Thr 92, Tyr 360, Glu 123, Arg 124	Thr 92, Tyr 360, Solvent (2005, 2053, 2370, 2152, 2371)
Akuammine pose 3	123.8	Asp 415, Tyr 520, Tyr 523, Gly_2000, Solvent (2569, 2568, 2569)	Asp 415, His 383, Tyr 520, His 513, Tyr 523, Glu 384, Val 380, Ala 354, His 353, Phe 457, Phe 527,		-60.3	Asn 85, Ala 85, Tyr 62, Ile 88, Glu 123, Thr 92, Trp 59	Thr 92, Asn 85, Solvent (2055, 2152, 2110)
Lisinopril	-107.4	Tyr 523, His 353, Tyr 520, Lys 511, solvent (2409, 2568, 2569, 2393, 2567, 2392, 2409, 2570)	Ala 354, Glu 384, Glu 411, Tyr 523, His 353, His 513, Lys 511, Tyr 520, Gln 281, Glu 162	Zn-701A, Glu 411, Glu 384, His 383, His 387, Glu 162, His 513, Lys 511, Asp 377			



(a)



(b)



(c)

Figure 4: Lineweaver-Burk plots (a,b,c) of angiotensin-1-converting enzyme (20 μ) without or with Akuammine

Compounds with total surface area of 60 is said to be highly non polar and it can cross the blood brain barrier while those above 90 are generally too polar. Akuammine had 93.5 which made it unsuitable to cross the blood brain barrier. Solubility is also an important factor that is very paramount to drug development, Compounds with LogP below 2 is generally acceptable, Akuammine had Log octanol/water partition coefficient of 1.5, Lipinski drug like test is 1, Lipinski violation count was 0. This is a clear indication that showed that the compound is a good drug candidate because the Log P is above one and the molecular weight is below 500 g/mol.

Conclusion

Akuammine showed inhibition on angiotensin-1-converting enzyme (ACE1), therefore Akuammine could be a lead compound in the discovery of drugs for hypertension.

Conflict of Interest

The authors declare no conflict of interest.

Authors' Declaration

The authors hereby declare that the work presented in this article is original and that any liability for claims relating to the content of this article will be borne by them.

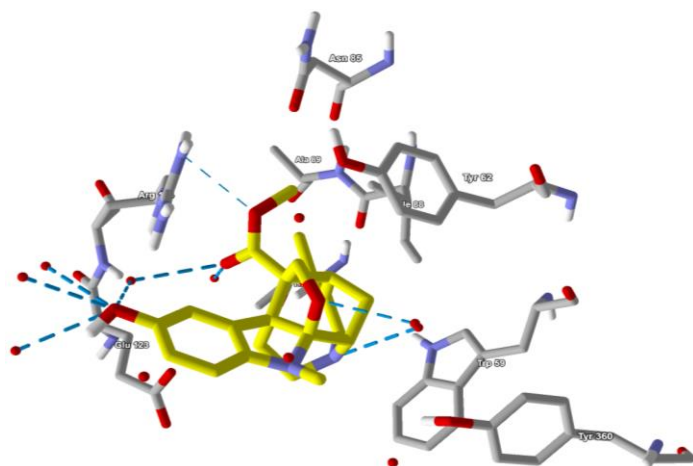


Figure 5: The binding of pose of Angiotensin-I-Converting Enzyme {ACE1 (PDB: 1O86)} with Akuammine (PDB: 1O8)

Funding

This research is partly funded by TERTFUND grant

Acknowledgements

Author, OOC appreciates the Department of Chemistry and Atmospheric Physics and The Federal University of Technology, Akure for the support given towards the success of this research.

References

- World Health Organisation (2019), <https://www.who.int/news-room/fact-sheets/detail/hypertension>.
- Navar LG. Physiology: hemodynamics, endothelial function, renin–angiotensin–aldosterone system, sympathetic nervous system. *J. Am. Soc. Hypertens.* 2014; 8(7): 519-524. <https://doi.org/10.1016/j.jash.2014.05.014>
- Fang L, Geng M, Liu C, Wang J, Min W, Liu J. Structural and molecular basis of angiotensin-converting enzyme by computational modeling: Insights into the mechanisms of different inhibitors. *PLoS One.* 2019; 14(4): e0215609. [10.1371/journal.pone.0215609](https://doi.org/10.1371/journal.pone.0215609)
- Fountain JH, Kaur J, Lappin SL. Physiology, Renin Angiotensin System.. In: StatPearls [Internet]. Treasure Island (FL): StatPearls Publishing. 2023; <https://www.ncbi.nlm.nih.gov/books/NBK470410/>
- Lacaille-Dubois MA, Franck U, Wagner H. Search for potential Angiotensin Converting Enzyme (ACE)-inhibitors from plants. *Phytomedicine.* 2001; 8(1): 47-52. <http://www.urbanfischer.de/journals/phytomed>
- Page MR. The JNC 8 Hypertension Guidelines: An In-Depth Guide. *Am. J. Manag. C.* 2014; 20(SP 1).
- James PA, Oparil S, Carter BL, Cushman WC, Dennison-Himmelfarb C, Handler J, Smith SC. Evidence-based guideline for the management of high blood pressure in adults: report from the panel members appointed to the Eighth Joint National Committee (JNC 8). *J. Amer. Med. Assoc.* 2014; 311(5): 507-520. doi:10.1001/jama.2013.284427
- Pinargote P, Guillen D, Guarderas JC. ACE inhibitors: upper respiratory symptoms. *Case Rep.* 2014; bcr2014205462. <http://dx.doi.org/10.1136/bcr-2014-205462>
- Abdulazeez AM, Ajiboye OS, Wudil AM, Abubakar H. Partial purification and characterization of angiotensin converting enzyme inhibitory alkaloids and flavonoids from the leaves and seeds of *Moringa oleifera*. *J. Adv. Biol. Biotechnol.* 2016; 5(2): 1-11. Doi: [10.9734/JABB/2016/21974](https://doi.org/10.9734/JABB/2016/21974)
- Olaleye MT, Adegboye OO, Akindahunsi AA. Antioxidant and antihypertensive investigation of seed extract of *Parinari curatellifolia*. *Medicinal plants: phytochemistry, pharmacology and therapeutics.* 2010; 1: 363-377.
- Crown OO, Olayeriju OS, Kolawole AO, Akinmoladun AC, Olaleye MT, Akindahunsi AA. Mobola plum seed methanolic extracts exhibit mixed type inhibition of angiotensin I-converting enzyme in vitro. *Asian Pac. J. Trop. Biomed.* 2017; 7(12): 1079-1084. Doi: [10.1016/j.apjtb.2017.10.009](https://doi.org/10.1016/j.apjtb.2017.10.009)
- Holmquist B, Bünning P, Riordan JF. A continuous spectrophotometric assay for angiotensin converting enzyme. *Anal. biochem.* 1979; 95(2): 540-548. Doi: [10.1016/0003-2697\(79\)90769-3](https://doi.org/10.1016/0003-2697(79)90769-3)
- Bull HG, Thornberry NA, Cordes MH, Patchett AA, Cordes EH. Inhibition of rabbit lung angiotensin-converting enzyme by N alpha-[(S)-1-carboxy-3-phenylpropyl] L-alanyl-L-proline and N alpha-[(S)-1-carboxy-3-phenylpropyl] L-lysyl-L-proline. *J. Biol. Chem.* 1985; 260(5): 2952-2962. Doi:
- Bradford MM. A rapid and sensitive method for the quantitation of microgram quantities of protein utilizing the principle of protein-dye binding. *Anal. biochem.* 1976; 72(1-2): 248-254. Doi: 10.1006/abio.1976.9999.
- Thomsen R, Christensen MH. MolDock: A new technique for high-accuracy molecular docking. *J. Med. Chem.* 2006; 49: 3315-3321. Doi: [10.1021/jm051197e](https://doi.org/10.1021/jm051197e)
- Halgren TA. Merck molecular force field. I. Basis, form, scope, parameterization, and performance of MMFF 94. *J. Comput. Chem.* 1996; 17: 490-519. Doi: 10.1002/(SICI)1096-987X(199604)17:5/6<490::AID-JCC1>3.0.CO;2-P.
- Gerber PR, Müller K. MAB, a generally applicable molecular force field for structure modelling in medicinal chemistry. *J. Comput. Aid. Mol. Des.* 1995; 9: 251-268. Doi: [10.1007/BF00124456](https://doi.org/10.1007/BF00124456)
- Wang J, Cieplak P, Kollman PA. How well does a restrained electrostatic potential (RESP) model perform in calculating conformational energies of organic and biological molecules? *J. Comput. Chem.* 2000; 21(12): 1049-1074. Doi: 10.1002/1096-987X(200009)21:12<1049::AID-JCC3>3.0.CO;2-F
- Case DA, Darden TA, Cheatham TE, Simmerling CL, Wang J, Duke RE, Luo R., Crowley M, Walker RC, Zhang W, Merz KM, Wang B, Hayik S, Roitberg A, Seabra G, Kolossváry I, Wong KF, Paesani F, Vanicek J, Wu X, Brozell SR, Steinbrecher T, Gohlke H, Yang L, Tan C, Mongan J, Hornak V, Cui G, Mathews DH, Seetin MG, Sagui C, Babin V, Kollman PA. AMBER 10, University of California, San Francisco. 2008.
- Lewin G, Le Ménez P, Rolland Y, Renouard A, Geisen-Crouse E. Akuammine and dihydroakuammine, two indolomonoterpene alkaloids displaying affinity for opioid receptors. *J. Nat. Prod.* 1992; 55(3): 380-384. Doi: [10.1021/np50081a017](https://doi.org/10.1021/np50081a017)
- Jang JH, Jeong SC, Kim JH, Lee YH, Ju YC, Lee JS. Characterisation of a new antihypertensive angiotensin I-converting enzyme inhibitory peptide from *Pleurotus cornucopiae*. *Food chem.* 2011; 127(2): 412-418. Doi: [10.1016/j.foodchem.2011.01.010](https://doi.org/10.1016/j.foodchem.2011.01.010)
- Hetthiweha SK, Hemar Y, Rupasinghe HP. Flavonoid-rich extract of *Actinidia macrosperma* (a wild kiwifruit) inhibits angiotensin-converting enzyme in vitro. *Foods.* 2018; 7(9): 146. Doi: [10.3390/foods7090146](https://doi.org/10.3390/foods7090146)
- Fu H, Rodriguez GA, Herman M, Emrani S, Nahmani E, Barrett G, Figueroa HY, Goldberg E, Hussaini SA, Duff KE. Tau Pathology Induces Excitatory Neuron Loss, Grid Cell Dysfunction, and Spatial Memory Deficits Reminiscent of Early Alzheimer's Disease. *Neuron.* 2017; 93(3): 533-541. Doi: [10.1016/j.neuron.2016.12.023](https://doi.org/10.1016/j.neuron.2016.12.023)